

Particle tracking in a gap of aquatic vegetation meadow

G. Ciruolo¹, C. Costa¹, G. B. Ferreri^{1*}, A. M. Folkard² and A. Maltese¹

¹ *Dipartimento di Ingegneria Idraulica e Applicazioni Ambientali, Università degli Studi di Palermo (Department of Hydraulic Engineering and Environmental Applications, University of Palermo), Viale delle Scienze – Ed. 8, 90128 Palermo, Italy*

² *Catchment & Aquatic Processes, Lancaster Environment Centre, Lancaster University, United Kingdom*

*Corresponding author, e-mail giofer@idra.unipa.it

ABSTRACT

Aquatic vegetation considerably affects the flow field in water bodies, with an increasing influence as the depth decreases. As a consequence, vegetation also affects the suspended particle transport. Meadows of *Posidonia oceanica* are widespread in the Mediterranean Sea in inshore sandy beds shallower than 40 m. This plant is constituted by a tuft of very thin and flexible ribbon-like leaves about 1 cm wide and up to 1.5 m long; the meadow areal density can reach 1000-1200 plants per square metre. Frequently, such vegetation meadows are not continuous but are interrupted by sandy strips. These discontinuities noticeably affect the flow field and can actually act as particle traps. In this paper, the flow field measured in past experiments is used for studying the behaviour of a gap in an artificial *Posidonia oceanica* canopy towards suspended particle transport. A simple particle tracking model assuming no-slip condition and random velocity fluctuations is adopted. A large number of single-particle tracking was performed taking into account several release elevations of particles as well as a number of settling velocities. The examination of the whole tracks allows one to recognize the particle fate as the simulation parameters vary. In spite of the model simplifying assumptions, the study gives useful indications on the behaviour of a gap towards the suspended particle transport.

KEYWORDS

Aquatic vegetation; suspended transport; particle tracking; turbulence; shallow water.

INTRODUCTION

Aquatic vegetation meadows considerably affect flow field and flow resistance with as more dramatic effects as shallower is the water column. Vegetal mantle, in fact, on the one hand considerably reduces the velocity in the lower flow layer with respect to a bare bottom, as well as, on the other hand, it interacts with the flow causing intense eddy activity near the vegetation top (Ghisalberti and Nepf, 2002; Ciruolo *et al.*, 2007; Okamoto and Nezu, 2009). The flow velocity reduction inside the canopy is caused by conversion of mean kinetic energy into turbulent kinetic energy effected by the plants (Nepf, 1999); along with the mean velocity reduction, a decrease in turbulent length scale occurs. In marine environment, the reduction of mean velocities and turbulent length scale effects the bed protection from erosion by heavy seas, tidal and currents. The conversion of mean kinetic energy into turbulent kinetic energy, moreover, dampens the total sea kinetic energy available for shore erosion.

Besides mitigating bed erosion, vegetation also reduces suspended transport through two distinct mechanisms which can occur individually or simultaneously (Purich, 1996): direct



Figure 1. *Posidonia oceanica* meadows: the left panel shows a meadow at the natural habitat of the lagoon *Stagnone di Marsala* (12°28'E, 37°52'N, Sicily, Italy), the right panel shows a meadow discontinuity.

capture and sedimentation. The former consists in removal of suspended particles from the flow as they collide with leaves and stems being capturing by adhesion to a sticky periphyton layer (Palmer *et al.*, 2004); the latter is due to the lower velocities which cause more particles to sink while resuspension is considerably reduced (Gacia *et al.*, 1999). The importance of both the mechanisms in reducing suspended transport is documented in the technical literature (*e. g.*, Agawin and Duarte, 2002).

The sediments transported by the flow can have a nature both inorganic (sand, silt, etc.) and biological (pollens, aquatic micro-fauna, animal and vegetal fragments, etc.). The size and density of suspended particles can vary considerably and this has consequences on the fate of particles. Inorganic sediments usually have a diameter ranging between 2 and 2000 μm with a density of about $2650 \text{ kg}\cdot\text{m}^{-3}$, whereas typical biological particles have a diameter between a few micrometres and some millimetres and a density between a little more than 1000 and about $1400 \text{ kg}\cdot\text{m}^{-3}$ (*e. g.*, Purich, 1996).

In addition to the effects on erosion and sediment transport, aquatic vegetation meadows play an important role in biological equilibrium of marine environment, as they produce a considerable oxygen quantity as well as they are ideal habitats for breeding and growing of numerous animal species, many of which find nourishment in sediments captured by meadows.

In inshore waters of the Mediterranean Sea, up to 40 m deep, *Posidonia oceanica* (Figure 1, left panel) is widespread. This phanerogam consists of roots, a short stem (“rhizome”) and leaves. The rhizome grows in both the vertical and the horizontal directions, forming “mattes”, peculiar terrace formations constituted by a weave of many root beds filled by sediments entrapped within them. The leaves are ribbon-like and very flexible, about 1 cm wide and up to 1.5 m long; they are arranged in tufts, usually composed of six leaves with age and length decreasing from outside to inside. *Posidonia oceanica* settles on sandy beds forming vast meadows even very dense (usually from 500 up to 1000-1200 $\text{plant}\cdot\text{m}^{-2}$). Frequently, *Posidonia oceanica* meadows are not continuous but vegetated areas alternate with sand strips (Figure. 1, right panel). The presence of such discontinuities in the meadows noticeably affects the flow field and, consequently, the sediment transport. The effects of a *meadow discontinuity* on the sediment transport has been little studied up to now, although it is an important topic recognizing whether a discontinuity operates as a “trap” for the sediments having passed the upstream vegetated area or, on the contrary, as a “source” of suspended sediments for the flow downstream of the discontinuity.

Some experiments were carried out at the *Dipartimento di Ingegneria Idraulica e Applicazioni Ambientali* (Dept. of Hydraulic Engineering and Environmental Applications) of the University of Palermo (Italy), in a flume equipped with an artificial canopy of *Posidonia oceanica* presenting a gap. The experiments, actually, aimed at studying the flow field within

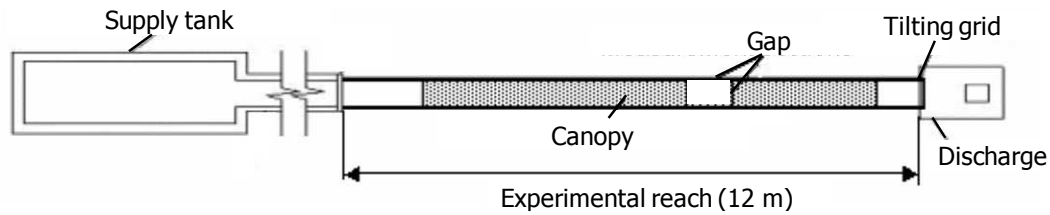


Figure 2. Experimental flume with the discontinuous canopy placed within the final 12 m reach.

the gap as well as in the upstream and downstream canopy stretches (Maltese *et al.*, 2005; Maltese *et al.*, 2007). In the present paper the experimental flow field of one of those runs is adopted as the base to simulate the tracks of single particles within the canopy gap. The aim is to examine the fate of particles as the settling velocity and the initial height of the particle vary as well as, consequently, to recognize whether the gap mainly operates as a trap or a source of sediments.

In the following sections, the experimental equipment is firstly described; then the instantaneous velocities, measured in the selected measurement points, are processed by an interpolation technique to describe more closely the whole velocity field; the model adopted for particle tracking is presented in the next section; finally, the results of the simulations as the settling velocity and the initial height of the particle vary are discussed.

EXPERIMENTAL EQUIPMENT

The experimental set up was presented in detail by Maltese *et al.* (2007), here only the essential information is given. The experiments were performed in a level laboratory flume 26.2 m long (Figure 2) having a rectangular section $77.2 \times 60.0 \text{ cm}^2$. The bottom was marble while the bearing structure was part iron and part concrete; in the final 12 m reach, used for the experiments, the walls were glass. The flume was supplied by a concrete tank which received water from two pipes, of 350 and 150 mm, each equipped with a flow-rate meter. At the flume downstream end there was a tilting grid for control of sub-critical flows.

In the final 12 m reach an artificial *Posidonia oceanica* canopy was placed, which was 9.60 m long and started 1.70 m from the reach beginning (Fig. 3, left panel). The plants were made by assembling six strips of low density polyethylene 1 cm wide and 0.2 mm thick (Fig. 3, middle panel). The outer couple of leaves was 50 cm long, the middle one 25 cm and the inner one 12.5 cm. The plants were arranged on steel-wooden panels, each 76.7 cm wide (Fig. 3, right panel). The planimetric distribution chosen for the plants produced an areal density of 1037

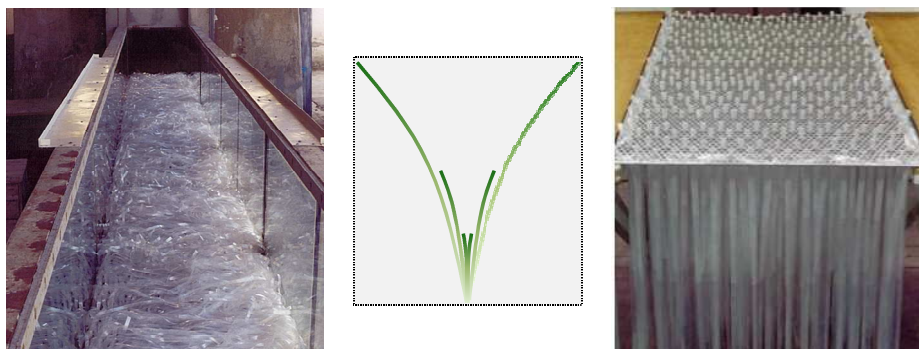


Figure 3. Artificial canopy: view of the canopy upstream of the gap (left panel), sketch of a plant, made by assembling six polyethylene strips (middle panel), and plants arranged in a pre-pierced steel plate before the latter was fixed to a wooden panel (right picture).

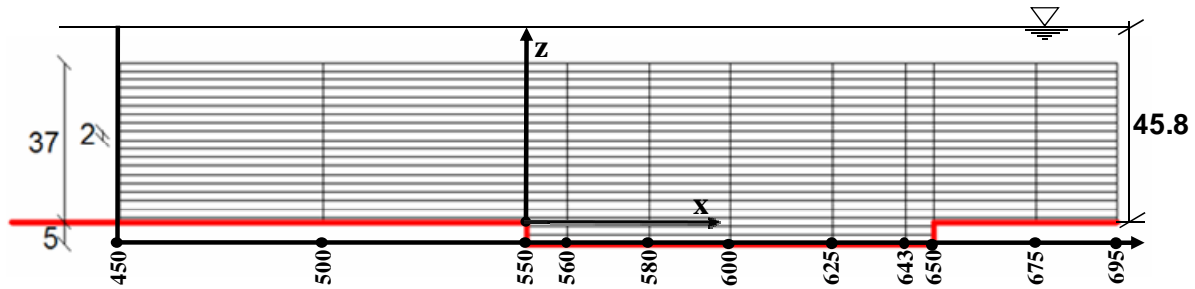


Figure 4. Sketch of the vegetated stretch between secs. 450 and 695 showing the gap (between secs. 550 and 650) as well as the gauging verticals and horizontal in the stretch.

plants·m⁻². Upstream and downstream, the vegetated bed was linked to the marble bottom of the flume by concrete slides.

Between the sections located at 550 and 650 cm from the canopy beginning no panel was set, so that a 1 m gap was realized (Figure 4); the drop between the canopy bed and the flume marble bottom was 5 cm. The drop mirrored the natural situation as in the vegetated areas the bed is higher than in the unvegetated ones because of the rhizome weave and the sediment accumulation. In Figure 4 the sections are indicated by their distance in centimetres from the canopy beginning.

The run whose measurements are used in this paper had a depth $h = 45.8$ cm, taken in a section located a little downstream of the gap, and an average velocity in the same section $U = 5.5$ cm·s⁻¹. The measurements regarded the velocities along several verticals on the flume axis, between sections 150 and 695. The verticals were chosen at steps of 50 cm between sections 150 and 550, whereas between sections 550 and 695 variable steps were adopted according to Figure 4. Along each vertical the measurement points were taken at steps of 2 cm (Figure 4). Instantaneous velocities were gauged by a down-looking 3D ultrasonic instrument of *ADV* type made by Nortek. Since *ADV* takes measurements in a sample volume located about 5 cm far from the probe, which had to be immersed below the free surface, in practice the velocities could be acquired up to 37 cm over the vegetated bed. At each point the acquisition time was ≈ 4 min with a frequency of 25 Hz. The frame reference was assumed as in Figure 4, with the x -axis being stream wise and the z -axis vertical and upward.

In order to restrict gauging problems due to leaves being in physical contact and pressing up against the probe, for taking measurements along a given vertical the probe was first placed at the lowest gauging location, after the foliage had been opened, and it was then moved upwards up to the highest location. When a time series exhibited excessive noises (which was judged subjectively from real-time plots displayed during data collection) it was discarded and the acquisition was repeated. According to Maltese *et al.* (2007), specific experiments proved that, although polyethylene moving leaves could act as scatterers of the *ADV* signal, reliable water velocity measurements could be obtained by filtering out data having correlation values lower than 70% and signal to noise ratio $SNR < 15\%$.

DATA PROCESSING AND FLOW FIELD CHARACTERISTICS

The instantaneous measurements of the velocity components u , v and w , respectively along x , y and z , gauged at each node were first filtered on the basis of the signal to noise ratio and of the correlation parameter, in order for the disaggregated measurements to be discarded. As the measurements were taken along the flume axis the component v was practically null. The filtered data were then used to determine the time-averaged values \bar{u} and \bar{w} , the fluctuations u' and w' , the standard deviations and the frequency distributions of u' and w' , the Reynolds stress $\overline{u'w'}$ as well as to carry out the quadrant analysis. For the sake of brevity, some results

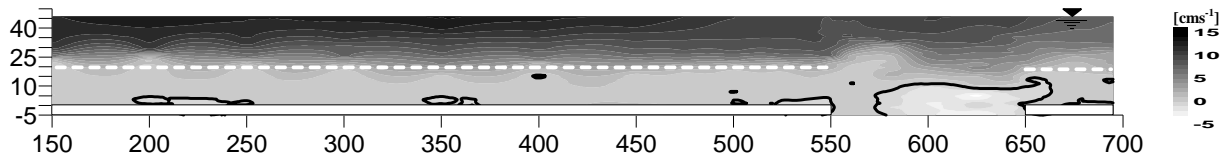


Figure 5. Representation by means of a gray scale of time-averaged velocity \underline{u} [$\text{cm}\cdot\text{s}^{-1}$]; the dotted white line indicates the mean height of the inflected vegetation.

only of the turbulence analysis are reported here while more extensive analysis of the turbulence characteristics will be made in further papers.

The above point data were then interpolated in space to obtain values in the nodes of a closer grid than the gauging one, for which we chose a 2 cm x -step and a 1 cm z -step. The point data were also extrapolated up to the free surface adopting the same grid. Among the interpolation techniques we selected that based on the *Radial Basis Function* (Franke, 1982) with the *Multiquadric method*, as it is an interpolator of type “exact” having a basis kernel function analogous to variograms in Kriging, which defines an optimal set of weights to be assigned to the point data when interpolating the value at a grid node. Following a semi-variogram analysis, anisotropy was set equal to 2, while, according to Carlson and Foley (1991), the smoothing factor was chosen between the average sample spacing and one-half the average sample spacing. Figure 5 shows the distribution of the mean velocity \underline{u} , whose intensity is highlighted by means of a gray scale. The horizontal bold broken line indicates the mean height of the vegetation. The bold lines contour the zones having negative \underline{u} (*i. e.*, towards upstream). The picture shows that inside the vegetation considerably lower velocities occur compared to those outside the vegetation, which is consistent with results of the technical literature (*e. g.*, Nepf and Vivoni, 2000; Ciraolo *et al.*, 2006; Ciraolo *et al.*, 2008). In the first part of the gap the low-velocity zone noticeably expands but then it contracts. As the flow experiences the effects of the downstream vegetated reach and it tends to reassume the upstream velocity distribution, which occurs after section 695 reported in the figure, the low-velocity zone again expands upwards.

Figure 6 shows the velocity vector field in the gap and in its upstream and downstream neighbourhoods. In the second part of the gap a large clockwise eddy is observed, which accounts for the upwards expansion of the low-velocity zone in the first part of the gap as well as for the velocities directed upstream close to the bottom. As further consequences of the eddy, at the gap beginning the upper flow “rears up” to climb over the eddy as well as the related velocities noticeably increase compared with those of the vegetated reach. In the highest layer, however, the velocities are analogous to those in the vegetated reach.

The analysis of the distributions of the Reynolds stress and the dominant quadrants (not reported for brevity) leads to results consistent with the aforesaid ones. In particular, an increase in the Reynolds stress is observed within the gap, with a peak close to the eddy centre, as well as sweep events are dominant in most part of the gap while ejection events only in the upper part of the gap.

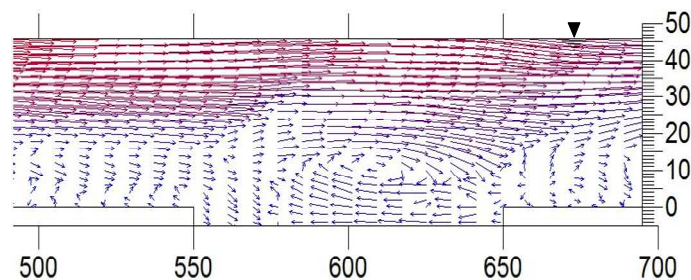


Figure 6. Velocity vector field in and around the gap.

STUDY OF THE GAP BEHAVIOUR

The interpolated flow field was used to investigate the behaviour of the gap towards the suspended sediment transport. Simulation of suspended particle transport is, in general, a very complex topic as this phenomenon depends on the flow characteristics (turbulence included) as well as on the particle characteristics (geometrical, physical, chemical, etc.) and the particle behaviour during the transport (decay, coalescence, etc.) (Shirolkar *et al.*, 1996). Particle transport and turbulence actually influence each other as the mere presence of a particle locally modifies the turbulence as well as a big particle mass load may effect global modification of the turbulence; furthermore, a large particle number density makes particle-particle interactions (such as collisions and coalescence) have to be taken into account (Berlemont *et al.*, 1998). By contrast, as the concentration of particles is very low, their influence on the global turbulence is negligible; particle-particle interactions can be ignored and the whole particle transport can be studied as the “sum” of transport of the single particles (Shirolkar *et al.*, 1996). As long as the particles are small enough, they follow the fluid motion and, in practice, no slip velocity there exists between the two phases, which, therefore, can be treated as a sole homogeneous flow with appropriately changed physical properties (Durst *et al.*, 1984).

Modelling of the particle trajectories

It is known (*e. g.*, Durst *et al.*, 1984; Shirolkar *et al.*, 1996) that suspended particle transport can be modelled following two approaches, Lagrangian and Eulerian. The Eulerian models treat the particulate phase as a *continuum* as if two fluids are present within the flow field. The concentration of the “particle fluid” in the “carrier fluid” has to be considered. The particle transport is monitored by the variations in the concentration within each fixed differential control volume as the particle fluid flows through the control volumes. No trajectories of single particles are carried out. The Lagrangian models, by contrast, treat the particulate phase as it actually is, as a *discrete* system, and each particle is tracked as it moves in the flow field. At each time, the position reached by a particle is a function of the point from where the particle originated and of the time elapsed and it accounts for particle history effects. These models highlighting the non-continuum behaviour of the particulate phase are particularly right for simulating transport of diluted particulate phases.

In the present paper aimed at recognizing the *qualitative* behaviour of the gap rather than at quantifying the sediment transport along the gap, a simple Lagrangian model was adopted. The particle concentration was assumed to be low enough so that inter-particle collisions as well as changes in the measured properties of the turbulent flow field due to the particle transport could be neglected. The particle characteristics were just globally taken into account by the settling velocity V_s , which for small particles is given by the Stokes’ law

$$V_s = \frac{1}{18} \frac{(\rho_p - \rho_w)}{\mu} g D^2 \quad (1)$$

where ρ_p is the particle density, ρ_w the water density, μ the water viscosity, g gravity acceleration and D the particle diameter. A no-slip condition was assumed for the particle motions driven by the flow field, which is acceptable for small particles with a low inertia to drag force ratio (Willgoose, 1997). In this scheme, the only cause of deviation of the trajectory of a sediment particle from that of a water particle, both originating from the same point at the same time, was the gravity force through the settling velocity V_s . The particle motion during each time step was split in three stages: the first stage was the particle advection due to the local mean flow velocity; the second one was caused by gravity; the third stage accounted for the local velocity fluctuation. The no-slip condition concerned the first

and the third stages. The velocity fluctuations u' and w' were determined randomly on the basis of their experimental statistic properties at the point reached by the particle. The coordinates at time t_{i+1} of the particle which at time t_i passed at point A were given by

$$x_{i+1} = x_{A,i} + \Delta t (u_{A,i} + M_x u'_{SD_{A,i}}) \quad (2)$$

$$z_{i+1} = z_{A,i} + \Delta t (w_{A,i} + M_z w'_{SD_{A,i}} - V_s) \quad (3)$$

were Δt is the time step between times t_i and t_{i+1} , u'_{SD} and w'_{SD} are the standard deviations of the fluctuations u' and w' respectively, M_x and M_z are random weights generated by means of the frequency distribution of the experimental velocity fluctuations; the subscript A indicates a quantity at point A and the subscript i a quantity at time t_i . Actually, at each gauging point in the gap, the frequency distributions of the normalized fluctuations u'/u'_{SD} and w'/w'_{SD} were practically coincident each other; indeed, the frequency distributions proved also to be practically *unchanged* over all the gauging points. Therefore, a *sole* mean frequency curve was adopted for u'/u'_{SD} and w'/w'_{SD} over the whole gap. This result indicates a strong correlation exists among the statistical properties of the velocity fluctuations in the points of the gap. This interesting issue will be stressed in a further paper. At each time step, two distinct random values in the range (0, 1) were generated which produced the weights M_x and M_z . A constant time step $\Delta t = 0.15$ s was assumed for all the realizations, without accounting for eddy lifetime and eddy transit time at each point reached by the particle (Shirolkar *et al.*, 1996). The model further assumed the settling velocity to be independent on the local velocity fluctuations, whereas theoretical as well as experimental studies showed that this velocity in vertically oscillating flow is actually lower as compared with that in still water (Willgoose, 1997). The model adopted is conceptually rough but it is simple to handle; however, it appears to be sufficient for a qualitative analysis of the gap behaviour.

Particle tracking and gap behaviour

Many trajectory realizations were carried out releasing particles at the first section of the gap (sec. 550). One particle only was released each time at a release height h_r varying between 1 and 40 cm from the canopy bottom, at steps of 1 cm. The settling velocity V_s was assumed equal to 0.2, 0.4, 0.6, 0.8, 1, 1.5 and 2 $\text{cm}\cdot\text{s}^{-1}$. Note that, according to the Stokes' law (Eq. 1), a higher settling velocity does not imply a higher particle density. For each couple of h_r and V_s values, 1000 realizations were carried out to account for stochastic effects on the trajectories. However, it is to be noted that no considerable deviations there occurred from a realization to another; therefore, the results of the simulations will be shown taking a "typical" realization only for fixed h_r and V_s values. Each realization went on until the particle reached the boundary of the computational domain (*i. e.*, either the upstream or downstream gap end sections or the gap bottom or the free-surface). If the particle reached the gap bottom it was considered definitively *settled* as no resuspension was considered.

Figure 7 shows, as examples, the trajectories simulated as h_r varied, for V_s fixed at 2, 1 and 0.2 $\text{cm}\cdot\text{s}^{-1}$. With the highest settling velocity $V_s = 2$ $\text{cm}\cdot\text{s}^{-1}$ (Figure 7, upper panel) all the particles settle, most of them in the first third of the gap and only a few in the second half. Particles released at h_r up to 20 cm (which is about the height of the vegetation inflected) follow trajectories having a roughly constant slope, which is consistent with the low and quasi-constant flow velocities in that part of the gap (Figure 6). The particles released above 20 cm experience eddy effects and follow more or less curved trajectories. The middle panel of Figure 7 relates to the settling velocity $V_s = 1$ $\text{cm}\cdot\text{s}^{-1}$. Decreasing in the settling velocity

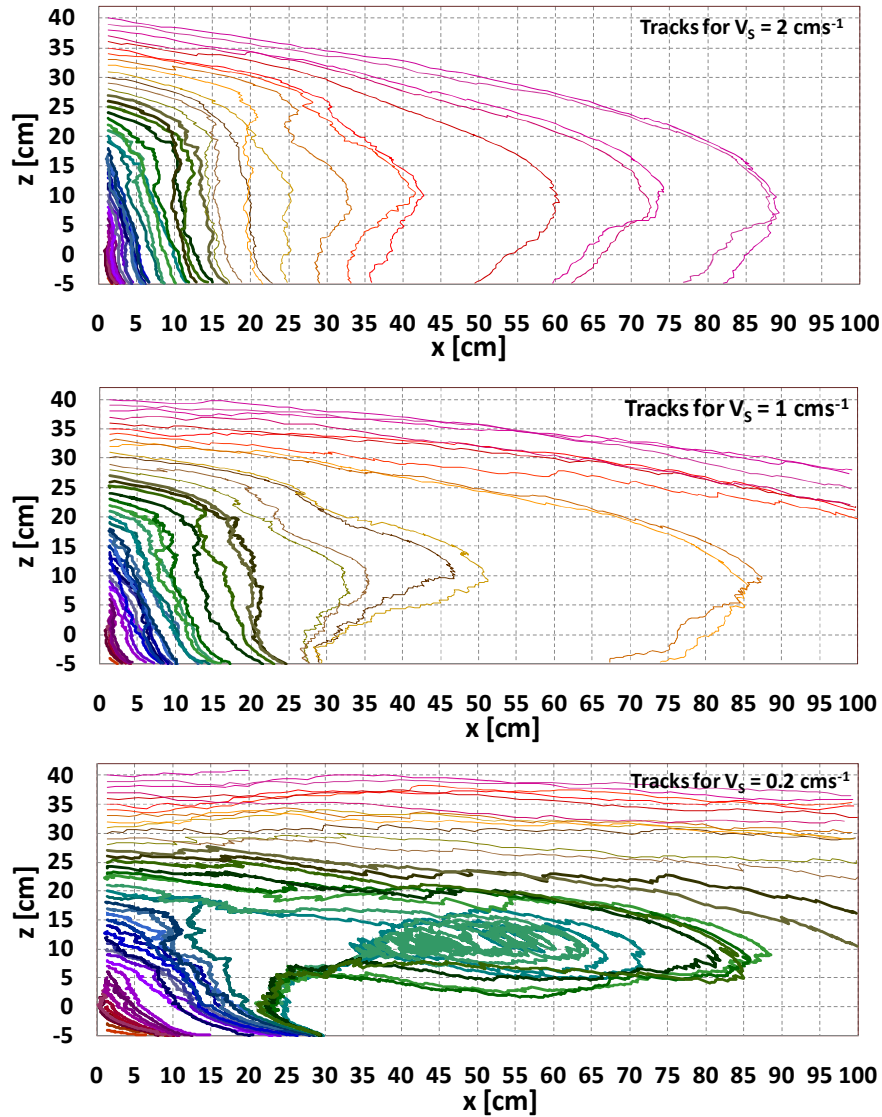


Figure 7. Typical trajectories simulated assuming the settling velocity V_s equal to $2 \text{ cm}\cdot\text{s}^{-1}$ (upper panel), $1 \text{ cm}\cdot\text{s}^{-1}$ (middle panel) and $0.2 \text{ cm}\cdot\text{s}^{-1}$ (lower panel).

allows the particles released at the higher h_r now to reach the downstream vegetated stretch. However, most of the particles settle in the gap, the most part again within the first third whereas only two in the second half. Note that, because of the random simulated turbulence, some couples of close tracks intersect several times. Further decreasing of V_s down to the minimum value considered of $0.2 \text{ cm}\cdot\text{s}^{-1}$ (Figure 7, lower panel) produces a considerable increase in the number of particles reaching the downstream vegetated stretch. Most of the particles, however, again settle in the gap and namely within the first third of the gap. The particles released up to $h_r = 18 \text{ cm}$ follow trajectories roughly rectilinear, whereas those released at $h_r = 19\text{-}25 \text{ cm}$ are entrained by the eddy, in which they remain entrapped at most for a few rounds before go out and then settle on the bottom.

In short, the numerous simulations performed showed that both the settling velocity and the release height considerably affect the particle fate. Only the lower settling velocities make it possible particles to reach the downstream vegetated stretch, but this occurs only for the higher release heights for which the particles are driven downstream by the upper flow layer, which get over the eddy and is characterized by more intense velocities than in the lower part of the flow. Particles released at median heights can be entrapped in the eddy for the lower settling velocities only but within one or a few rounds they go out and settle. Particles

released up to about the vegetation height, which move in the “vegetation shade” characterized by very low velocities, always settle following roughly rectilinear trajectories. On the whole, the realizations showed that the most frequent particle fate is settling within the gap, mainly in the first third of it. According to this result, sediment deposition has to be expected close to the end of the upstream canopy. Of course, for practical applications detailed indications are necessary on the actual distribution of the particles in the first section of the gap as well as on their characteristics, which implies targeted field investigations to be carried out.

CONCLUSIONS

The behaviour of a gap in aquatic vegetation meadow towards suspended sediment transport was examined by means of numerical simulations. The simulations were carried out on the basis of the flow field measured in past laboratory experiments in a flume with an artificial canopy of *Posidonia oceanica*. A close description of the flow field was first obtained by means of interpolation in space of the point measurements. A simple Lagrangian model was adopted for sediment transport, which assumed a so diluted particulate phase that inter-particle interactions could be neglected and no changes in the global turbulence were produced; the model also assumed a so small particle diameter that no-slip condition could be adopted. Three stages were considered for the particle motion during each time step, respectively accounting for advection, gravity and turbulence. The turbulent fluctuations were determined randomly on the basis of their experimental statistical properties. The particle characteristics were globally accounted for by means of the settling velocity. Many particle tracking realizations were carried out releasing single particles at the first section of the gap for several values of the release height and the settling velocity.

The whole realizations showed that only particles having the lower settling velocities and released at the higher heights reached the downstream vegetated stretch. Most of the particles, by contrast, settled in the gap, usually in the first third of it. As these particles were released at heights below the vegetation top they settled following roughly rectilinear trajectories; when released above the vegetation top, the particles experienced the effects of the big eddy which formed in the gap and followed noticeably curvilinear trajectories.

In conclusion, despite the conceptual approximations the model adopted allowed us to have some useful indications for understanding the gap operates as a *sediment trap*. Of course this knowledge has to be integrated with field results concerning the actual distribution along the vertical as well as the physical characteristics of particles in marine environment.

Next steps should concern model improvement in order for dynamics of particle to be accounted for (elimination of *no-slip* hypothesis) and more appropriate turbulent fluctuations to be given at each time step which, although being random, should exhibit satisfactory coherence both in time and in space as particle goes along its trajectory. Generation of coherent fluctuations by appropriate processing of no-synchronized point measurements is a prominent topic for particle tracking.

ACKNOWLEDGMENTS

The authors of the present paper contributed equally to this work, and their names appear in alphabetical order. The writers wish to thank Dr. Giovanni Lombardo and Dr. Eleanor Cox for their dedication and systematic work in setting up the experimental equipment and carrying out the measures as well as for making the measurements available for the present paper.

REFERENCES

- Agawin, N. S. R. and Duarte, C. M. (2002). Evidence of direct particle trapping by a tropical seagrass meadow. *Estuaries*, 25(6A), 1205-1209.
- Berlemont, A., Chang, Z. and Gouesbet, G. (1998). Particle Lagrangian tracking with hydrodynamic interactions and collisions. *Flow, Turbulence and Combustion*, 60, 1-18.
- Carlson, R. E., and Foley, T. A. (1991). The parameter R^2 in multiquadric interpolation. *Computers and Mathematics with Applications*, 21(9), 29-42.
- Ciraolo, G., Ferreri, G. B. and La Loggia, G. (2006). Flow resistance of *Posidonia oceanica* in shallow water. *Journal of Hydraulic Research*, 44(2), 189-202.
- Ciraolo, G., Ferreri, G. B. and La Loggia, G. (2007). Flow resistance of a very dense *Posidonia oceanica* grassland in shallow water. *Proc. of the 5th International Symposium on Environmental Hydraulics – ISEH V*, Tempe, Arizona (U.S.A.), Dec. 4-7, 1-6, CD-ROM.
- Ciraolo, G., Ferreri, G. B. and La Loggia, G. (2008). Influence of *Posidonia oceanica* meadow density on flow resistance in shallow waters. *Proc. of the 2nd International Symposium on Shallow Flows*, Hong Kong, China, Dec. 8-12, 1-6, CD-ROM.
- Durst, F., Milojevic, D. and Schönung, B. (1984). Eulerian and Lagrangian predictions of particulate two-phase flows: a numerical study. *Applied Mathematical Modelling*, 8, 101-115.
- Franke, R. (1982). Scattered data interpolation: test of some methods. *Mathematics of Computations*, 33(157), 181-200.
- Gacia, E., Granata, T. C. and Duarte, C. M. (1999). An approach to measurement of particle flux and sediment retention within seagrass (*Posidonia oceanica*) meadows. *Aquatic Botany*, 65(1-4), 255-268.
- Ghisalberti, M. and Nepf, H. M. (2002). Mixing layers and coherent structures in vegetated aquatic flows. *Journal of Geophysical Research*, 107(C2), 1-11.
- Maltese, A., Folkard, A. M., Ciraolo, G., Cox, E. and Ferreri, G. B. (2005). On the influence of flexible vegetation on flow fields in shallow water: a flume experiment. *Proc. of the 9th Workshop on Physical Processes in Natural Waters*, Lancaster, United Kingdom, Sep. 4-6, 195-202.
- Maltese, A., Cox, E., Folkard, A. M., Ciraolo, G., Lombardo, G. and La Loggia, G. (2007). Laboratory measurements of flow and turbulence in discontinuous distributions of ligulate seagrass, *ASCE, Journal of Hydraulic Engineering*, 133(7), 750-760.
- Nepf H. M. (1999). Drag, turbulence, and diffusion in flow through emergent vegetation. *Journal of Water Resources Research*, 35(2), 479–489.
- Nepf H. M. and Vivoni E. R. (2000). Flow structure in depth-limited, vegetated flow. *Journal of Geophysical Research*, 105(C12), 28,547-28,557.
- Okamoto, T. and Nezu, I. (2009). Turbulence structure and “Monami” phenomena in flexible vegetated open-channel flows. *Journal of Hydraulic Research*, 47(6), 798-810.
- Purich A. (2006). The capture of suspended particles by aquatic vegetation. Environmental Engineering Project Dissertation, School of Environmental Systems Engineering, The University of Western Australia.
- Palmer, M. P., Nepf, H. N. and Petterson, T. J. R. (2004). Observations of particle capture on a cylindrical collector: Implications for particle accumulation and removal in aquatic systems”. *Limnology and Oceanography*, 49(1), 76-85.
- Shirolkar, J. S., Coimbra, C. F. M. and McQuay, M.Q. (1996). Fundamental Aspects of Modeling Turbulent Particle Dispersion in Dilute Flows. *Progress in Energy and Combustion Science*, 22, 363-399.
- Willgoose, G. (1997). A hydrodynamic particle tracking algorithm for simulating settling of sediment. *Mathematics and Computers in Simulation*, 43, 343-349.